Geometry Dependent Microwave Absorption Properties in Carbonaceous Materials over X-Band Frequencies (8.2-12.4 GHz) for Stealth Applications

Lokesh Saini[1], Priyambada Sahoo[2], Raj Kumar Jani[1], Ambesh Dixit*[2]

[1]*Stealth Technologies Division, Defence Laboratory, Defence Research & Development Organisation (DRDO), Ratanada, Jodhpur, 342011, India*
[2]*Advanced Materials and Devices (A-Mad) Laboratory, Department of Physics, Indian Institute of Technology Jodhpur, Karwar, Jodhpur, 342037, India*

Volume 1, Issue 5, October 2024
Received:6 September, 2024; Accepted: 16 October, 2024
DOI: https://doi.org/10.63015/5C-2438.1.5

**Correspondence Author- ambesh@iitj.ac.in*

Abstract: Carbonaceous materials of two different types, viz. spherical nano carbon black (NCB) powder (Brunauer-Emmett-Teller (BET) surface area ~1400 m^2/g) and multiwalled carbon nanotube (MWCNT) (BET surface area ~75 m^2/g), have been impregnated in room temperature vulcanized (RTV) silicon rubber matrix to study the effect of geometries of filler particles on microwave absorption characteristics, over X-band frequencies (8.2 -12.4 GHz). The rubber-based composites are prepared by dispersion of NCB and MWCNT fillers in the liquid rubber with loading fractions ranging from 0.3-0.9 wt% and 1.1-1.7 wt%, respectively. The dielectric loss tangent ($\tan\delta_e$) profiles were evaluated for the filler-loaded rubber composites at different concentrations. The calculated Reflection loss (RL) profiles suggest that NCB-based rubber provides maximum RL value, $(RL)_{max}$ ~ -20 dB (99.00 % absorption), at a lower filler concentration of 0.5 wt%, as compared to MWCNT. However, the MWCNT-based rubber composite shows enhanced $(RL)_{min}$ values of ~ -29 dB (~99.99% absorption) due to multiple scattering phenomena. The identified NCB and MWCNT-based rubber-based MW absorbers have potential stealth applications for military aerial vehicles.

Keywords: Stealth, DC conductivity, rubber composites, loss tangent, reflection loss

1. Introduction: With the escalating progress in Microwave (MW)/Radar technology during the last few decades, serious concerns are also emerging in society, viz., the unkind effect of MW radiation on human health, detection of fighter aircraft by enemy Radars during wartime operations, communicational interferences/clutters among MW instrumentations, etc., [1]–[3]. Therefore, the development of Microwave Absorbing Materials (MAMs) and their products in the forms of sheets/coatings/structures having desired properties picked up the interest of scientific community to suit the requirements. The electromagnetic parameters of these materials, viz. complex permittivity ($\varepsilon^*=\varepsilon'-j\varepsilon''$), complex permeability ($\mu^*=\mu'-j\mu''$), and conductivity (σ) play a critical role in microwave absorption, which decide the type of absorption (magnetic/dielectric) and MW frequency band coverage [4]. Among the other MW frequency bands, X-band (8.2-12.4 GHz) has been widely used in the defence sector for the detection, tracking, and surveillance of objects requiring airborne objects' protection for their survivability [5].

Different types of materials, viz. metal flakes [6], ferrites [7], [8], carbonyl iron [9], ferroelectrics [10], core-shell materials [11], [12], etc., have been explored by researchers due to their wide frequency range of MW absorption as well as superior reflection loss values. However, higher loading fractions of filler material in host matrices are reported to achieve the optimum MW absorption in composites made of these MAMs. The implication of higher filler loading in the matrix translates into high density, weight penalty, and lower mechanical strength of MW absorbing composites. Therefore, carbonaceous materials are being explored to fabricate lightweight & low-cost MW absorbers with thermal, mechanical, chemical, and environmental stability.[13]

Various carbonaceous materials, viz. graphene [14], carbon black [15], carbon nanotubes (CNTs) [16], graphite [17], carbon nanofibers (CNFs) [18], etc., have been used in resin [19], rubber [20], [21] and ceramic [22] matrices for their microwave absorption studies over the broad frequency range of 2-18 GHz. It is evident that carbonaceous materials, which are being used as MAMs, possess low density (range 1.6-2.3 g/cm^3) and high surface-to-volume ratio, which make them unsuitable for dispersion in resin/rubber matrix at higher filler loading, resulting in the formation of lumps, uneven distribution/segregation of filler powders, voids/crack in coating/sheets, etc. The inadequate dispersion of carbonaceous filler also resulted in inferior MW absorption properties. Therefore, selecting functional carbonaceous fillers and dispersing host matrix should be judicious to achieve the desired MW absorption properties at lower filler loading. The imaginary permittivity (ε_r") of the MW absorber represents the loss characteristics against incident MW signals, which is directly dependent on its DC conductivity (σ_{dc}) [23]. Hence, to achieve the desired conductivity of the composite absorber at a lower filler fraction, the conductive network of filler should be formed in an insulating host matrix, which eventually depends on the dispersion of filler particles in the matrix.

Resins/liquid rubbers are found to be better host matrix as compared to solid rubbers to attain the lower percolation threshold due to the attainment of strong crosslinking in rubbers during vulcanization, which prevents connection of long-range ordering of conducting filler in the host matrix [24]. Further, the filler particle shape, size, and surface area also determine the dispersion characteristics in resin matrices. In the present work, we have attempted to study the effect of particle shape, size, surface area, and aspect ratio on electromagnetic (EM) parameters and microwave absorption characteristics of the resin-filler composite. For the study, two different filler materials, viz. nano carbon black (NCB) powder with high surface area and multiwalled carbon nanotubes (MWCNT) with high aspect ratio, were dispersed in room temperature vulcanized (RTV) liquid silicon rubber in different filler fractions. Electromagnetic parameters of rubber composites were evaluated using a Vector Network Analyzer (VNA) over the X-band MW frequency range (8.4-12.4 GHz).

2. Experimental Details

2.1. Fabrication of Filler-Loaded Rubber Composite: Commercially available nanocarbon black and multiwalled carbon nanotubes were used as functional materials for MW absorption. Details of materials are given in Table 1. Two components of RTV silicone rubber (liquid rubber 95 wt%: catalyst 5 wt%) were used as a host matrix for the dispersion of carbonaceous filler materials. Initially, 95g of silicone rubber and 10 ml of solvent (o-Xylene) were mixed with the required filler powder and stirred for 30 minutes at 1200 RPM for its uniform dispersion in rubber. After thorough mixing, 5g of catalyst was added to the rubber-filler compound and stirred again for homogenization. The admixed compound was transferred uniformly into a die of size 100 mm × 100mm × 3mm and pressed into a hydraulic press at 01 Ton pressure to avoid any voids/pores in the composite structure. The rubber composite was removed from the die after 4 hours and kept in ambient for 24 hours for proper curing. The schematic for filler-loaded silicone rubber composite sheet fabrication is shown in Fig. 1. Further, a series of silicon rubber sheets were prepared by impregnating Nano Carbon Black (NCB) and multiwalled Carbon Nanotubes (CNT) as per the details provided in Table 2.

The filler-loaded silicon rubber sheets were cut in 22.86 × 10.16 mm (L × W) size for measurement through VNA over X-band frequencies (8.2 – 12.4 GHz).

Table 1: Details of Functional Materials

Sl. No.	Type of Material	Particle size (nm)	Particle Morphology	BET Surface area (m^2/g)	Source of Availability
1.	Nano Carbon Black (NCB) (Ketjenblack EC-600JD)	~5-10	Spherical	1400	AkzoNobel Functional Chemicals, USA
2.	Multiwalled Carbon Nano Tubes (MWCNT)	~5-10 (diameter)	Tubular Aspect ratio ~ 2000	75	Commercialized, Sigma Aldrich

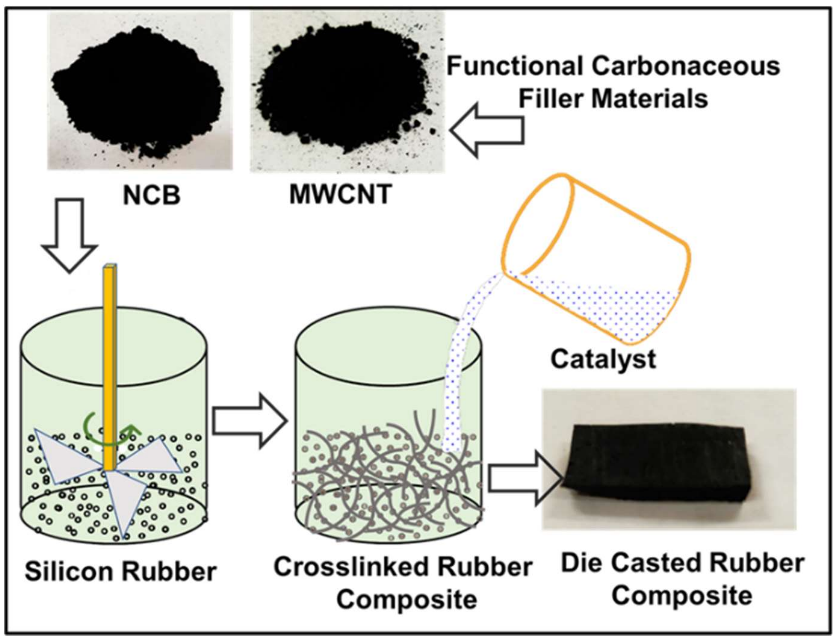

Figure 1. Schematic representation of fabrication of carbonaceous filler loaded silicon rubber composite sheet.

2.2. Characterization of Filler Materials and Rubber Composites: The crystal structure of NCB and CNT powders was investigated using an X-ray diffraction (XRD) system (Model: X'Pert Pro; Make: Philips) over the 2θ range of 20º-80º with incident radiation of Cu K_α (λ = 1.540 Aº). The morphology of both the powder samples was estimated using a Scanning Electron Microscope (SEM) (Model EVO5; Make: Oxford) for the filler powder samples. DC Conductivity of all the rubber composite samples was measured using a four-probe conductivity measurement set-up. EM parameters viz. complex permittivity and permeability of NCB/MWCNT loaded rubber composites sheets were estimated using a two-port waveguide transmission line technique with the help of Vector Network Analyzer (VNA) (Model: Keysight PNA;

Make: Keysight Technologies) over the frequency range 8.2-12.4 GHz. The reflection (S_{11}) and transmission (S_{22}) scattering parameters were measured through VNA, which were used in the estimation of complex permittivity (ε_r^*) and complex permeability (μ_r^*) using Nicolson-Ross-Weir (NRW) Algorithms [25].

Table 2: Details of Fabrication of Filler Loaded Silicon Rubber Sheet

Type of Material	Silicon resin (g)	Catalyst	Filler Amount (g)	Loading Fraction	Sample Nomenclature
Nano Carbon Black (NCB)	95	05	0.3	0.3 wt%	**NCB0.3**
	95	05	0.5	0.5 wt%	**NCB0.5**
	95	05	0.7	0.7 wt%	**NCB0.7**
	95	05	0.9	0.9 wt%	**NCB0.9**
Multiwalled Carbon Nanotubes (MWCNT)	95	05	1.1	1.1 wt%	**CNT1.1**
	95	05	1.3	1.3 wt%	**CNT1.3**
	95	05	1.5	1.5 wt%	**CNT1.5**
	95	05	1.7	1.7 wt%	**CNT1.7**

3. Results and Discussion

3.1. X-ray Diffraction Studies: The XRD pattern of nano carbon black (NCB) is shown in Fig. 2(a), which confirms the presence of hexagonal graphitic carbon peaks with (002) and (100) crystal planes in NCB [26]. The Fig. 2(b) shows the XRD pattern of MWCNT powder, where the intense characteristic graphite peak (002) at ~26° corresponds to tubular carbon atoms, and other peaks correspond to graphitized carbon peaks of (100) and (004) planes, respectively [27]. The XRD spectra of NCB and MWCNT powders confirm the phase purity materials, exhibiting no diffraction peak for other carbon allotropes.

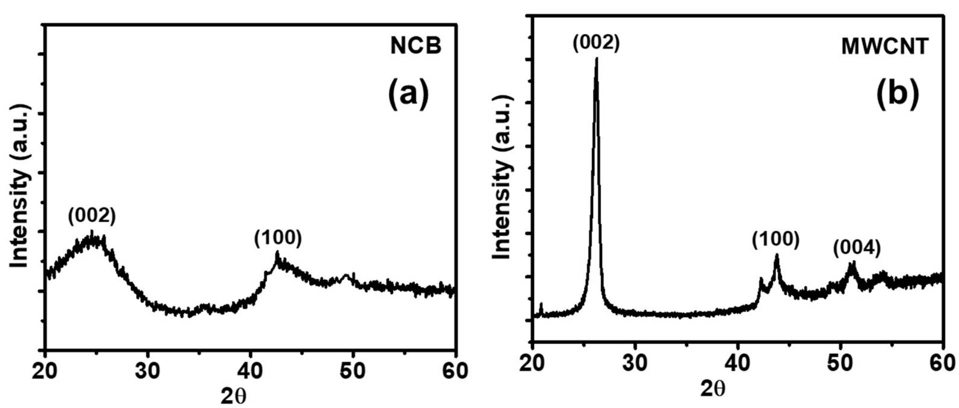

Figure 2. XRD spectra of (a) Nano carbon black (NCB) and (b) Multiwalled CNTs

3.2. Morphological Studies: Figure 3(a)-(b) show SEM micrographs of nanocarbon black powder (NCB) in different magnifications, which confirms the nearly spherical morphology. The SEM micrographs of MWCNT powder shown in Figure 3(c)-(d) confirm the fiber statures of the material.

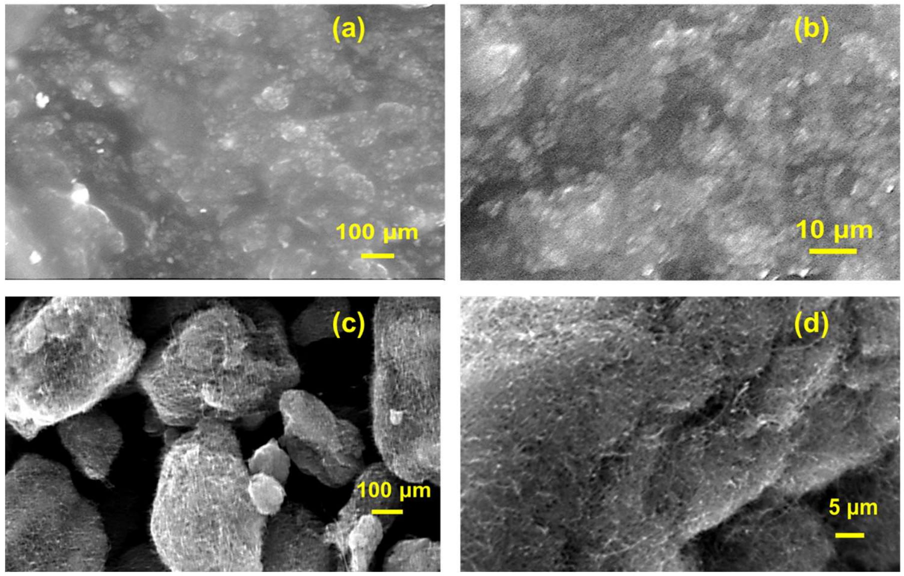

Figure 3. (a)-(b) SEM micrograph of NCB filler powder, (c)-(d) SEM micrograph of multiwalled CNT filler powder

3.3. DC Conductivity Studies: The DC conductivity (σ) values of NCB-rubber composites with filler loading in the 0.3-0.9 wt% range are shown in Fig. 4 (a). Initially, at lower NCB loading in NCB0.3 (0.3 wt%) & NCB0.5 (0.5 wt%) rubber composites, the σ values are found ~1.25 × 10^{-5} S/cm and 6.75x10^{-5} S/cm. With a further increase in NCB content to 0.7 wt% (NCB0.7), the values of σ increased to ~ 9.18 × 10^{-3} S/cm. However, with a further increase in NCB concentration to 0.9 wt% in the NCB0.9 composite sample, the σ increases drastically up to 0.17 S/cm due to forming a conducting network of nano carbon particles in silicon rubber composite [23]. Similarly, the MWCNT-loaded rubber composites CNT1.1 (1.1 wt%) & CNT1.3 (1.3 wt%) have σ values 1.95 × 10^{-4} S/cm and 5.86 × 10^{-5} S/cm, respectively. The 1.5 wt% MWCNT loaded sample (CNT1.5) exhibit σ ~ 1.06 × 10^{-5} S/cm. The increment of MWCNT filler powder up to 1.7 wt% in the composite, the σ value was increased abruptly up to 0.23 S/cm because of the formation of the conduction network. It is interesting to note that NCB-based rubber composite attains the DC conductivity value 0.17 S/cm at lower filler loading of 0.9 wt%, where the almost similar σ value in MWCNT-based rubber composite (0.23 S/cm) could be achieved at 1.7 wt% loading of filler powder. The main reason for this finding is attributed to the very high surface area of NCB powder (1400 m^2/g) as compared to MWCNT (75 m^2/g), which facilitates the formation of a conduction network in nanocarbon powder at a lower loading fraction as compared to MWCNT.

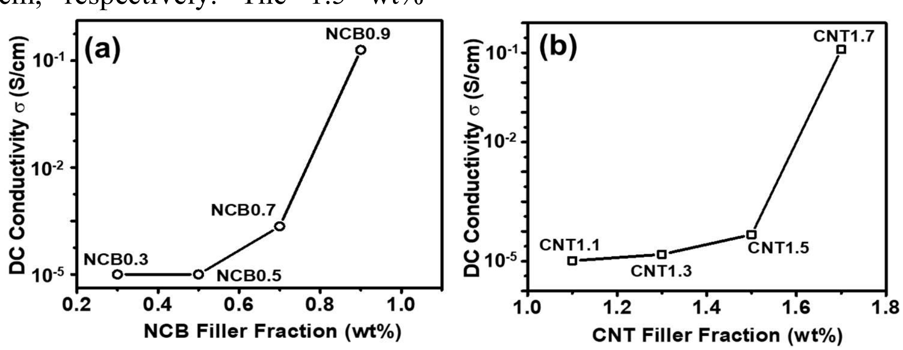

Figure 4. (a) Variation of DC conductivity with NCB filler loading in Si rubber (b) Variation of DC conductivity with MWCNT filler loading in Si rubber

3.4. Evaluation of EM Parameters: The EM parameters viz. real (ε_r') & imaginary (ε_r'') relative permittivity for NCB and MWCNT loaded rubber composites are shown in Fig. 5(a)-(d). The ε_r' values for 0.3 wt% NCB loaded composites NCB0.3 are almost constant ~ 6.5 over 8.2-12.4 GHz frequency range. The ε_r' values of NCB-based composites increase with enhancement in filler loading ~11.5±1 (NCB0.5), ~12.5±1 (NCB0.7) & ~14±2 (NCB0.9)] due to an increase in the effective concentration of conductive nano carbon filler in the insulating rubber matrix (Fig. 5a). These plots have dispersive nature with frequency variation. The real permittivity in such composites, in which conductive fillers (NCB & MWCNT) are dispersed in an insulating rubber matrix, is governed by Maxwel-Wagner type interfacial polarization. With the increase in the filler loading, the contribution of interfacial polarization also increases, which may be saturated beyond a threshold [15]. This effect may be more prominent beyond the frequency range of 10 GHz, as observed in Fig 5(a). Therefore, the ε_r' values for NCB0.7 & NCB0.9 are found to be almost similar. The imaginary permittivity (ε_r'') value of NCB/rubber composites, which is attributed to conduction losses, increases with increasing nanocarbon concentration due to an increase in DC conductivity (σ) governed by equation $\varepsilon''=\sigma/2\pi f\varepsilon_0$, where f is the frequency (GHz), and ε_0 is free space permittivity (8.85×10^{-12} F/m) [28]. The imaginary permittivity (ε_r'') values for NCB0.3, NCB0.5, NCB0.7 & NCB0.9 are observed ~1.6, ~5.3, ~7.8±0.2, and 13±1, respectively. Similarly, for MWCNT filler-loaded rubber composites CNT1.1-CNT1.7 (1.1 wt% to 1.7 wt%), the ε_r' values increase from ~15.4±0.9 (CNT1.1) to ~21±3 (CNT1.7) over 8.2-12.4 GHz frequency range, as shown in Fig. 5(c). The imaginary permittivity values of MWCNT-loaded rubber specimens also show an increasing trend with filler loading, viz. ~5±1 (CNT1.1), 8±1 (CNT1.3), 11±1 (CNT1.5) and 14±2 (CNT1.7) as depicted in Fig. 5(d).

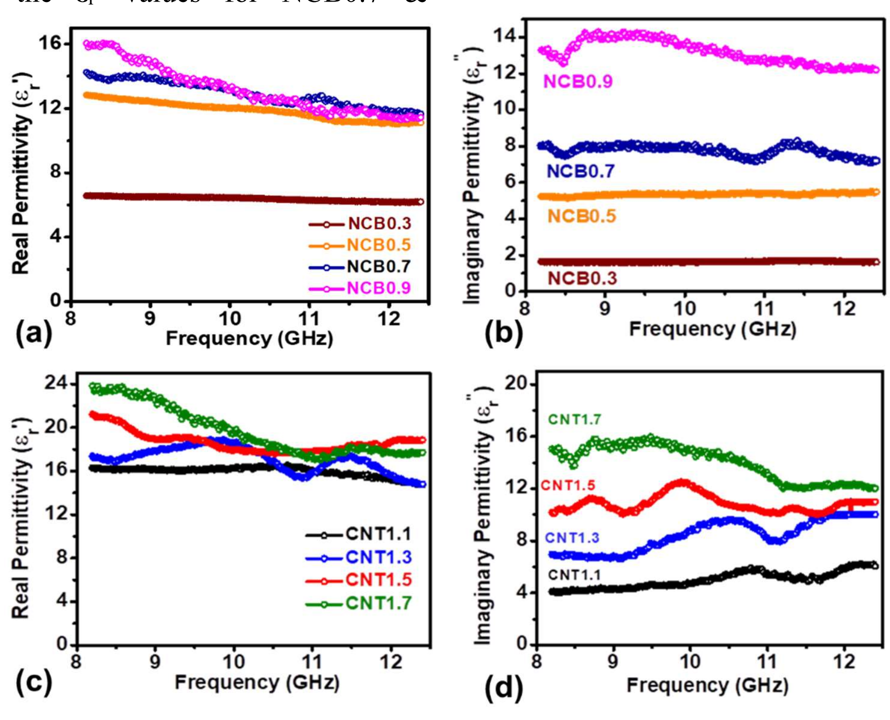

Figure 5. (a)-(b) Variation of relative real permittivity (ε_r') & imaginary permittivity (ε_r'') values for NCB filler loaded rubber composites (c)-(d) Variation of relative imaginary permittivity (ε_r'') values for MWCNT filler loaded rubber composites

The dielectric loss tangent $\tan\delta_e$ values, which are the ratio of ε_r" and ε_r' ($\tan\delta_e = \varepsilon_r''/\varepsilon_r'$) for NCB & MWCNT based rubber composites are plotted in Fig. 6(a)-(b). The $\tan\delta_e$ values for both the materials systems increase with the loading fraction of functional filler due to the enhancement of conduction loss in the rubber matrix. The NCB0.3, NCB0.5, NCB0.7 & NCB0.9 samples have corresponding $\tan\delta_e$ values ~0.25, ~0.45±0.05, ~0.55±0.05 and ~0.95±0.05, respectively. Whereas, $\tan\delta_e$ values for CNT1.1, CNT1.3, CNT1.5 & CNT1.9 samples are observed ~0.35±0.1, ~4.5±0.15, ~ 5.5±0.1 and ~7±0.1, respectively.

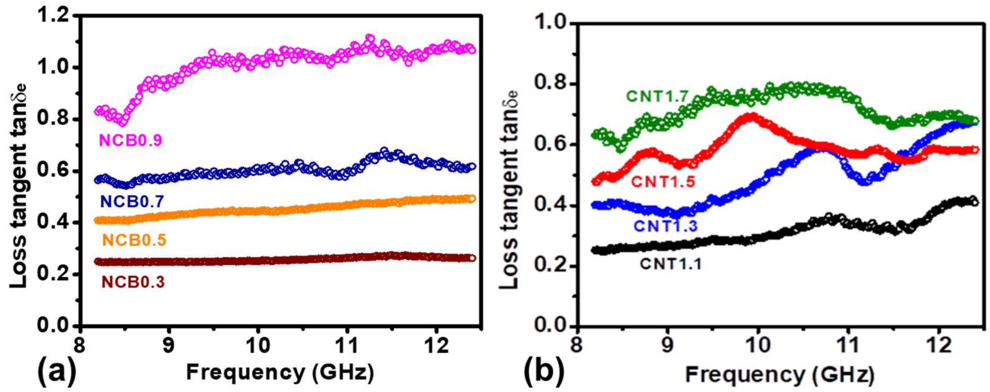

Figure 6. (a) Dielectric loss tangent ($\tan\delta_e$) plots for NCB loaded rubber composites (b) Dielectric loss tangent ($\tan\delta_e$) plots for MWCNT loaded rubber composites

3.5. Estimation of Reflection Loss (RL):

The reflection loss (RL) value, which is represented in decibels (dB), is the quantitative estimation of the MW absorption capability of any stealth product. The RL values can be calculated by Equation 1 [29].

$$RL\,(dB) = 20\log_{10}\left|\frac{\sqrt{\frac{\mu_r^*}{\varepsilon_r^*}}\tanh\left(\frac{j\,2\pi d}{\lambda}\sqrt{\mu_r^*\varepsilon_r^*}\right)-1}{\sqrt{\frac{\mu_r^*}{\varepsilon_r^*}}\tanh\left(\frac{j\,2\pi d}{\lambda}\sqrt{\mu_r^*\varepsilon_r^*}\right)+1}\right| \quad (1)$$

Where ε_r^* is complex permittivity, μ_r^* is complex permeability, d is absorber thickness, and λ is wavelength. Generally, the targeted RL value for any absorber used for stealth application is considered as minimum -10 dB or more (negative sign represents MW loss characteristics), which quantifies to 90% or more MW absorption capabilities. The matching thickness (d_m) where the RL values are found maximum is given by $d_m = \frac{c}{4f\sqrt{|\mu_r^*||\varepsilon_r^*|}}$, provides the critical design thickness for the fabrication of any stealth product. The RL plots for NCB-based absorbers NCB0.3-NCB0.9 are shown in Fig. 7(a)-(d). The NCB0.3 rubber composite has d_m value of 3.0 mm with a maximum RL(RL_{max}) value of ~ -13 dB at 10.3 GHz, shown in Fig.7(a). The RL profiles shift towards the lower frequency side with increasing absorber thickness, substantiating its reciprocal dependence. The NCB0.5 absorber shows improved RL performance as compared to NCB0.3, where (RL_{max}) value is ~ -20 dB at 9.8 GHz, at a reduced matching thickness of 2.2 mm, contributed by enhanced dielectric loss properties (Fig. 7(b)). Further, the absorption bandwidth for RL≥10dB is ~3.3 GHz over the entire X-band frequencies. With further increase in NCB content to 0.7 wt% in NCB0.7 absorber, the (RL_{max}) value decreases to ~ -18 dB at 10.2 GHz, having optimum thickness of 2.0 mm, however the absorption bandwidth is still found ~3.3 GHz (Fig. 7c). Interestingly, with still increase in NCB content to 0.9 wt% (NCB0.9), the $(RL)_{max}$ value decreases to ~ -6 dB with almost constant values throughout the frequency range of 8.2-12.4 GHz, as shown in Fig. 7(d). The loss tangent $\tan\delta_e$ values of this composite are maximum ~ 0.95±0.05 compared to other specimens; however, the RL values are still found inferior due to the onset of impedance mismatch of incident MW signals at the high conducting surface of the absorber [30].

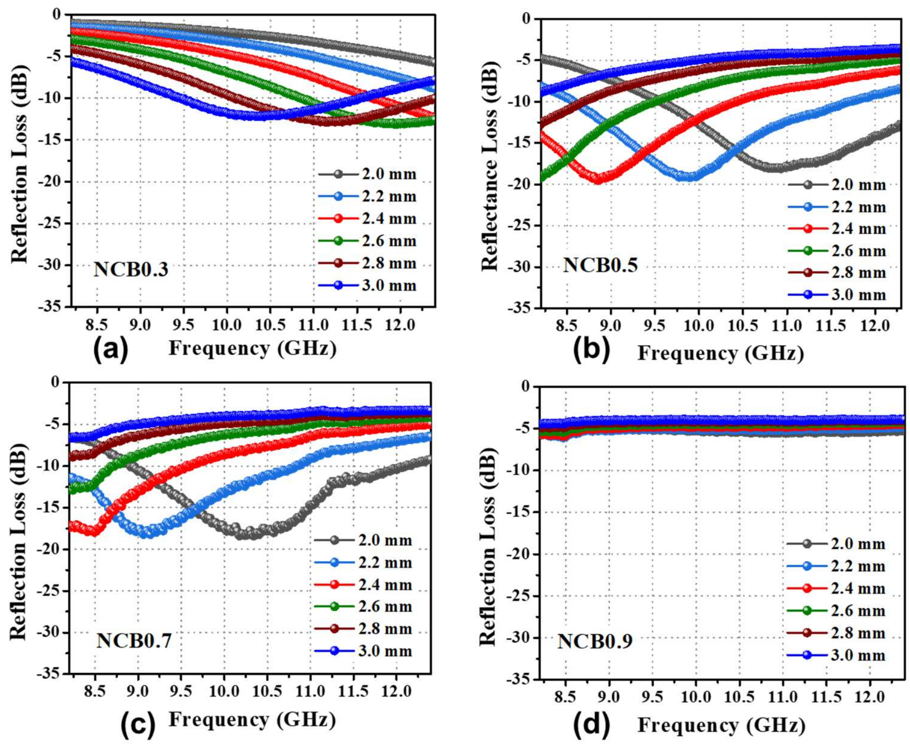

Figure 7. Frequency vs Reflection Loss (RL) plots for (a) NCB0.3 (b) NCB0.5 (c) NCB0.7 (d) NCB0.9

Figure 8 shows RL plots of MWCNT filler-based rubber absorbers with different loading ranges of 1.1-1.9 wt%. CNT1.1 sample has RL_{max} value ~ -18 dB at 8.5 GHz, having a matching thickness of 2.0 mm. The RL_{max} value of the CNT1.3 absorber significantly improved to ~ -29 dB at ~9.5 GHz with the same matching thickness of 2.0mm. The effective absorption bandwidth of this composition is at ~3 GHz at a thickness of 1.8 mm. The higher RL_{max} values in MWCNT-based rubber composite may be triggered by a high aspect ratio, which helps in multiple scattering of EM signals and enhances MW absorption. In the MWCNT-filled composites, the impedance mismatch was observed beyond the filler content of 1.3 wt%, which results in a lower RL_{max} value of ~ -10 dB in both CNT1.5 & CNT1.7 absorbers. Table 3 compares reported CB and MWCNT composite materials used for microwave absorption. Hence, these studies confirm that both high dielectric loss and impedance matching criteria should be met to achieve the optimum reflection loss values in MW absorbers. Further, the nanocarbon-based absorbers attain the desired MW absorption capabilities at lower filler loading than MWCNT-based composites due to the large surface area and proper dispersion attributed to spherical morphology. However, both the NCB and MWCNT-based rubber composites at optimized composition and thickness, viz. NCB0.5 and CNT1.3 are promising materials for stealth applications.

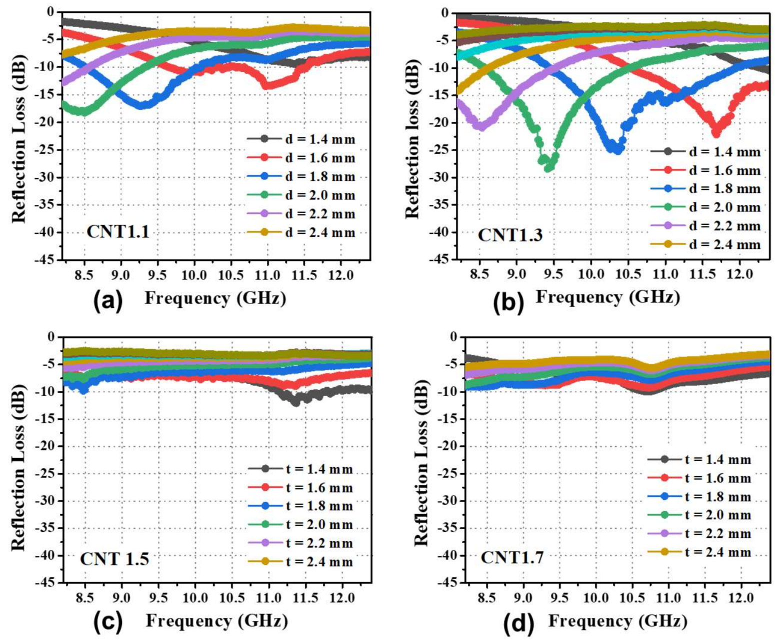

Figure 8. Frequency vs Reflection Loss (RL) plots for (a) CNT1.1 (b) CNT1.3 (c) CNT1.5 (d) CNT1.7

Table 3. The pristine carbonaceous (Carbon Black/Multiwalled CNT) and composite materials for MW absorption applications, borrowed from Ref [3].

Materials	Synthesis Route	Matrix	t (mm)	R_L (dB)	Frequency (GHz)	Bandwidth (GHz)	Ref.
CB	Commercial	Silicon Rubber	2.7 (X-band) 1.9 (Ku-band)	~ -21 (X-band) ~ -25 (Ku-band)	~ 10.0 (X-band) ~ 14 (Ku-band)	4 (X-band) 6 (Ku-band)	[23]
CB	Commercial	polypropylene	2.8 (X-band) 1.9 (Ku-band)	-62.6 (X-band) -39.15 (Ku-band)	10.64 (X-band) 15.08 (Ku-band)	4.56 (X-band) 5.63 (Ku-band)	[31]
CB & tetrapod like ZnO whiskers (T-ZnO)	Commercial	Epoxy Resin	3.0	-19.31	10.4	4.56	[32]
CB/SiC	Commercial	Epoxy Resin	2.0	~ -41	~ 9	6	[22]

CB/quartz glass fiber (SiO_{2f})	Commercial	Polyimide Rasin	1.6	-46.18	16.07	3.95	[33]
MWCNT	Commercial	Epoxy Resin	8	-29	11.5	3	[34]
MWCNT/CdS	chemical co-precipitation	Wax	1.5	-45	~15	-	[35]
Nano Carbon Black (NCB)	Commercialized, AkzoNobel Functional Chemicals, USA	Silicon Rubber	2.2	-20	9.8	3.3	This Work
MWCNT	Commercialized, Sigma Aldrich	Silicon Rubber	2.0	-29	9.5	3	This Work

4. Conclusion: Commercially available spherical-shaped Nano Carbon Black (NCB) (Particle size: 5-10 nm; BET surface area: 1400 m^2/g) and Multiwalled Carbon Nanotubes (MWCNT) (Diameter: 5-10 nm; BET surface area: $75m^2/g$; aspect ratio: 2000) were selected to study the effect of geometries of functional fillers on the MW absorption performance of rubber-based composites. XRD spectra confirm the phase purity of commercial carbonaceous fillers without the signature of any other carbon allotropes. SEM micrographs suggested nearly spherical and fiber structures of NCB and MWCNT filler powders. NCB and MWCNT-based rubber composites were synthesized by dispersing these filler powders in liquid silicon resin in the range of 0.3-0.9 wt% and 1.1-1.7 wt%, respectively. Further, DC conductivity (σ) measurement suggests that NCB filler-based rubber composites possess high values of σ~0.17 S/cm even at the lower filler concentration of 0.5 wt%, as compared to MWCNT filler, which obtains σ~0.23 S/cm at 1.1 wt% loading attributed to higher surface area. The EM parameters of both NCB and MWCNT-loaded rubber composites were evaluated over the frequency range of 8.2-12.4 GHz, and dielectric loss tangent $\tan\delta_e$ values increased with increasing filler loading. The calculated RL profiles suggest that 0.5 wt% NCB rubber composite (NCB0.5) shows optimized maximum RL values ~ -20 dB at the matching thickness of 2.2 mm due to complimentary participation of both dielectric loss and impedance matching. Further, the MWCNT-based composite with 1.1 wt% filler loading (CNT1.1) shows improved optimized RL values ~ -29 dB at the matching thickness of 2.0mm due to dielectric loss, impedance matching, and multiple reflections in the absorber medium. Both these absorbers have potential applications for the stealth treatment of airborne platforms.

Acknowledgement:

The authors thank Mr. R. V. Hara Prasad, Director of the Defence Laboratory, for his constant guidance and support for the present work. The authors are also thankful to Dr. R Nagarajan, Technology Director, Stealth Technology Division, and Dr. M. K. Patra, Defence Laboratory, for their fruitful suggestions during the work.

Conflict of Interest:
Authors declare No conflicts of interest.

References

[1] D. G. Xu, J. S. Liu, S. Luo, and P. Li, "Development Status and Trend of Stealth Technology of Tactical Missiles," J. Phys. Conf. Ser., 2460, **2023**, 012064

[2] H. Ahmad *et al.*, "Stealth technology: Methods and composite materials—A review," Polym. Compos., 40, **2019**, 4457–4472

[3] P. Sahoo, L. Saini, and A. Dixit, "Microwave-absorbing materials for stealth application: a holistic overview," Oxford Open Mater. Sci., 3, **2023**, itac012

[4] L. Cui, X. Han, F. Wang, H. Zhao, and Y. Du, "A review on recent advances in carbon-based dielectric system for microwave absorption," J. Mater. Sci., 56, **2021**, 10782–10811

[5] B. Zohuri, *Radar Energy Warfare and the Challenges of Stealth Technology*. Cham: Springer International Publishing, Book, **2020**.

[6] C. Zhang, J. Jiang, S. Bie, L. Zhang, L. Miao, and X. Xu, "Electromagnetic and microwave absorption properties of surface modified Fe-Si-Al flakes with nylon," J. Alloys Compd., 527, **2012**, 71–75

[7] S. M. Abbas, R. Chatterjee, A. K. Dixit, A. V. R. Kumar, and T. C. Goel, "Electromagnetic and microwave absorption properties of (Co^{2+}-Si^{4+}) substituted barium hexaferrites and its polymer composite," J. Appl. Phys., 101, **2007**, 074105

[8] L. Saini, M. K. Patra, R. K. Jani, G. K. Gupta, A. Dixit, and S. R. Vadera, "Tunable twin matching frequency (fm1 /fm2) behavior of $Ni_{1-x}Zn_xFe_2O_4$ /NBR composites over 2-12.4 GHz: A strategic material system for stealth applications," Sci. Rep., 7, **2017**,1–12

[9] K. S. Sista, S. Dwarapudi, D. Kumar, G. R. Sinha, and A. P. Moon, "Carbonyl iron powders as absorption material for microwave interference shielding: A review," J. Alloys Compd.,853, **2021**, 157251

[10] L. Vovchenko, O. Lozitsky, L. Matzui, V. Oliynyk, V. Zagorodnii, and M. Skoryk, "Electromagnetic shielding properties of epoxy composites with hybrid filler nanocarbon/$BaTiO_3$," Mater. Chem. Phys.,240, **2020**, 122234

[11] L. Wang *et al.*, "Synthesis and microwave absorption enhancement of graphene@Fe_3O_4@SiO_2@NiO nanosheet hierarchical structures," Nanoscale, 6, **2014**, 3157–3164

[12] X. Zhao *et al.*, "Excellent microwave absorption property of Graphene-coated Fe nanocomposites," Sci. Rep., 3, **2013**, 3421

[13] F. Ruiz-Perez, S. M. López-Estrada, R. V. Tolentino-Hernández, and F. Caballero-Briones, "Carbon-based radar absorbing materials: A critical review," J. Sci. Adv. Mater. Devices, 7, **2022**, 100454

[14] F. Meng *et al.*, "Graphene-based microwave absorbing composites: A review and prospective," Compos. Part B Eng., 137, **2018**, 260–277

[15] S. K. Kwon, J. M. Ahn, G. H. Kim, C. H. Chun, J. S. Hwang, and J. H. Lee, "Microwave absorbing properties of carbon black/silicone rubber blend," Polym. Eng. Sci., 42, **2002**, 2165–2171

[16] X. Chen, H. Liu, D. Hu, H. Liu, and W. Ma, "Recent advances in carbon nanotubes-based microwave absorbing composites," Ceram. Int., 47, **2021**, 23749–23761

[17] D. J. Gogoi, "Microwave absorber based on encapsulated expanded graphite-silicone composite as meta-'atom' for X-band application," J. Electromagn. Waves Appl., 34, **2020**, 1444–1459

[18] H. Breiss, A. El Assal, R. Benzerga, C. Méjean, and A. Sharaiha, "Long Carbon Fibers for Microwave Absorption: Effect of Fiber Length on Absorption Frequency Band," Micromachines, 11, **2020**, 1081

[19] X. Lv, S. Yang, J. Jin, L. Zhang, G. Li, and J. Jiang, "Preparation and Electromagnetic Properties of Carbon Nanofiber/Epoxy Composites," J. Macromol. Sci. Part B, 49, **2010**, 355–365

[20] S. Vinayasree *et al.*, "Flexible microwave absorbers based on barium hexaferrite, carbon black, and nitrile rubber for 2-12GHz applications," J. Appl. Phys., 116, **2014**, 024902

[21] J. H. Kaiser, "Microwave evaluation of the conductive filler particles of carbon black-rubber composites," Appl. Phys. A Solids Surfaces, 56, **1993**, 299–302

[22] X. Liu, Z. Zhang, and Y. Wu,

"Absorption properties of carbon black/silicon carbide microwave absorbers," Compos. Part B Eng., 42, 2011, 326–329
[23] R. K. Jani, L. Saini, and S. R. Vadera, "Size dependent percolation threshold and microwave absorption properties in nano carbon black/silicon rubber composites," J. Appl. Phys.,131, **2022**, 044101
[24] R. K. Jani, L. Saini, and S. R. Vadera, "Rheological Dependence on Dielectric and Microwave Absorption Properties of Carbon Black/Rubber Nanocomposites Over 6–18 GHz," J. Electron. Mater., 53, **2024**, 3187–3198
[25] A. M. Nicolson and G. F. Ross, "Measurement of the Intrinsic Properties Of Materials by Time-Domain Techniques," IEEE Trans. Instrum. Meas., 19, 1970, 377–382
[26] R. Ramaraghavulu, V. K. Rao, K. C. Devarayapalli, K. Yoo, P. C. Nagajyothi, and J. Shim, "Green synthesized AgNPs decorated on Ketjen black for enhanced catalytic dye degradation," Res. Chem. Intermed., 47, **2021**, 637–648
[27] R. Atchudan, A. Pandurangan, and J. Joo, "Effects of nanofillers on the thermo-mechanical properties and chemical resistivity of epoxy nanocomposites," J. Nanosci. Nanotechnol., 15, **2015**, 4255–4267.
[28] L. Wang *et al.*, "Recent progress of microwave absorption microspheres by magnetic-dielectric synergy," Nanoscale, 13, **2021**, 2136–2156.
[29] F. Qin and C. Brosseau, "A review and analysis of microwave absorption in polymer composites filled with carbonaceous particles," J. Appl. Phys., 111, **2012**, 061301.
[30] L. Saini *et al.*, "Impedance engineered microwave absorption properties of Fe-Ni/C core-shell enabled rubber composites for X-band stealth applications," J. Alloys Compd., 869, **2021**, 159360.
[31] L. Lei, Z. Yao, J. Zhou, B. Wei, and H. Fan, "3D printing of carbon black/polypropylene composites with excellent microwave absorption performance," Compos. Sci. Technol., 200, **2020**, 108479.
[32] H. Qin, Q. Liao, G. Zhang, Y. Huang, and Y. Zhang, "Microwave absorption properties of carbon black and tetrapod-like ZnO whiskers composites," Appl. Surf. Sci., 286, **2013**, 7–11.
[33] J. Dong *et al.*, "Dielectric and microwave absorption properties of CB doped SiO2f/PI double-layer composites," Ceram. Int., 44, **2018**, 14007–14012.
[34] M. K. Naidu, K. Ramji, B. V. S. R. N. Santhosi, T. Shami, H. B. Baskey, and B. Satyanarayana, "Enhanced Microwave Absorption of Quartic Layered Epoxy-Mwcnt Composite for Radar Applications," Adv. Compos. Lett., 26, **2017**, 096369351702600.
[35] X. X. Wang, M. M. Lu, W. Q. Cao, B. Wen, and M. S. Cao, "Fabrication, microstructure and microwave absorption of multi-walled carbon nanotube decorated with CdS nanocrystal," Mater. Lett., 125, **2014**, 107–110.